Terahertz confocal microscopy with a quantum cascade laser source

Ugo Siciliani de Cumis,[1*] Ji-Hua Xu,[1] Luca Masini,[1] Riccardo Degl'Innocenti,[1] Pasqualantonio Pingue,[1] Fabio Beltram,[1] Alessandro Tredicucci,[1] Miriam S. Vitiello,[1] Pier Alberto Benedetti,[2] Harvey E. Beere,[3] and David A. Ritchie[3]

[1]*NEST, CNR-Istituto Nanoscienze and Scuola Normale Superiore, Piazza San Silvestro 12, I-56127 Pisa, Italy*
[2]*CNR-IPCF, Via G. Moruzzi 1, I-56124 Pisa, Italy*
[3]*Cavendish Laboratory, University of Cambridge, J J Thomson Avenue, Cambridge CB3 0HE, UK*
[*]*ugo.siciliani@sns.it*

Abstract: We report on the implementation of a confocal microscopy system based on a 2.9 THz quantum cascade laser source. Lateral and axial resolutions better than 70 μm and 400 μm, respectively, are achieved, with a large contrast enhancement compared to the non-confocal arrangement. The capability of resolving overlapping objects lying on different longitudinal planes is also clearly demonstrated.

OCIS codes: (140.5965) Semiconductor lasers, quantum cascade; (110.6795) Terahertz imaging; (180.1790) Confocal microscopy.

References and links

1. M. Tonouchi, "Cutting-edge terahertz technology," Nat. Photonics **1**, 97–105 (2007)
2. Y. Lee, *Principles of Terahertz Science and Technology* (Springer, 2009).
3. W. Chan, J. Deibel, and D. Mittleman, "Imaging with terahertz radiation," Rep. Prog. Phys. **70**, 1325–1379 (2007).
4. A. Fitzgerald, V. Wallace, M. Jimenez-Linan, L. Bobrow, R. Pye, A. Purushotham, and D. Arnone, "Terahertz pulsed imaging of human breast tumors," Radiology **239**, 533–540 (2006).
5. B. Hu and M. Nuss, "Imaging with terahertz waves," Opt. Lett. **20**, 1716–1718 (1995).
6. B. Ferguson and X. Zhang, "Materials for terahertz science and technology," Nat. Mater. **1**, 26–33 (2002).
7. D. Arnone, C. Ciesla, and M. Pepper, "Terahertz imaging comes into view," Phys. World **4**, 35–40 (2000).
8. D. Mittleman, R. Jacobsen, and M. Nuss, "T-ray imaging," IEEE J. Sel. Top. Quantum Electron. **2**, 679–692 (1996).
9. D. Mittleman, M. Gupta, R. Neelamani, R. Baraniuk, J. Rudd, and M. Koch, "Recent advances in terahertz imaging," Appl. Phys. B-Lasers O. **68**, 1085–1094 (1999).
10. V. Wallace, E. MacPherson, J. Zeitler, and C. Reid, "Three-dimensional imaging of optically opaque materials using nonionizing terahertz radiation," J. Opt. Soc. Am. A **25**, 3120–3133 (2008).
11. J. Zeitler, P. Taday, D. Newnham, M. Pepper, K. Gordon, and T. Rades, "Terahertz pulsed spectroscopy and imaging in the pharmaceutical setting-a review," J. Pharm. Pharmacol. **59**, 209–223 (2007).
12. J. Zeitler, Y. Shen, C. Baker, P. Taday, M. Pepper, and T. Rades, "Analysis of coating structures and interfaces in solid oral dosage forms by three dimensional terahertz pulsed imaging," J. Pharm. Sci. **96**, 330–340 (2007).
13. I. Sinka, S. Burch, J. Tweed, and J. Cunningham, "Measurement of density variations in tablets using x-ray computed tomography," Int. J. Pharm. **271**, 215–224 (2004).
14. M. Minsky, "Memoir on inventing the confocal scanning microscope," Scanning **10**, 128–138 (1988).
15. T. Corle and G. Kino, *Confocal Scanning Optical Microscopy and Related Imaging Systems* (Academic Press, 1996).
16. R. Webb, "Confocal optical microscopy," Rep. Prog.Phys. **59**, 427–471 (1996).
17. N. Zinovev and A. Andrianov, "Confocal terahertz imaging," Appl. Phys. Lett. **95**, 011114 (2009).

#170679 - $15.00 USD Received 15 Jun 2012; revised 10 Aug 2012; accepted 15 Aug 2012; published 10 Sep 2012

18. M. Salhi, I. Pupeza, and M. Koch, "Confocal thz laser microscope," J. Infrared Millim. Te. **31**, 358–366 (2010).
19. R. Köhler, A. Tredicucci, F. Beltram, H. Beere, E. Linfield, A. Davies, D. Ritchie, R. Iotti, and F. Rossi, "Terahertz semiconductor-heterostructure laser," Nature **417**, 156–159 (2002).
20. R. Degl'Innocenti, M. Montinaro, J. Xu, V. Piazza, P. Pingue, A. Tredicucci, F. Beltram, H. E. Beere, and D. A. Ritchie, "Differential Near-Field Scanning Optical Microscopy with THz quantum cascade laser sources," Opt. Express **17**, 23785–23792 (2009).
21. T. Losco, J. Xu, R. Green, A. Tredicucci, H. E. Beere, and D. A. Ritchie, "Thz quantum cascade designs for optimized injection," Physica E **40**, 2207 – 2209 (2008).
22. A. Siegman, M. Sasnett, and T. Johnston Jr, "Choice of clip levels for beam width measurements using knife-edge techniques," IEEE J. Quantum Elect. **27**, 1098–1104 (1991).
23. G. Xu, R. Colombelli, S. P. Khanna, A. Belarouci, X. Letartre, L. Li, E. H. Linfield, A. G. Davies, H. E. Beere, and D. A. Ritchie, "Efficient power extraction in surface-emitting semiconductor lasers using graded photonic heterostructures," Nature Commun. **3**, 952 (2012).

1. Introduction

Over the last two decades, photonic technologies for the terahertz (THz) region of the electromagnetic spectrum have experienced an extraordinary breakthrough, thanks to the progresses made in generation, manipulation and detection of radiation [1,2]. Many novel techniques have been pioneered, motivated in part by the vast range of practical applications such as high-speed communications, molecular spectroscopy, imaging in security controls, and medical diagnostics [2–4].

Most of the interest in THz imaging [5] resides in the peculiar ability of THz rays to deeply penetrate into non-polar and nonmetallic materials such as paper, plastic, clothes, wood and ceramics that are usually opaque at optical wavelengths. Such materials are frequently used for packaging and coating of many objects of common use, making THz imaging systems ideal tools for non invasive quality testing and for inspecting sealed containers [6–9]. Many complex organic molecules have characteristic absorption bands in the THz, while metal objects can also be easily identified due to their high reflectivity; these properties explain the high interest for security applications: weapons, explosives and illegal drugs can be easily identified even when concealed underneath typical wrapping and packaging materials [3, 10].

Moreover, because of the high absorption coefficient of water in the THz region, hydrated substances are easily differentiated from dried ones. This means that images of objects in which the water distribution is the relevant aspect can exhibit great contrast and quality. The high sensitivity of THz radiation to water is therefore particularly useful for medical applications because, in a biological system, small changes in water content could indicate crucial tissue differences, enabling people to distinguish between normal and damaged or cancerous tissue without recurring to invasive methods [3,4]. Pharmaceutical science is another field which benefits from the new possibilities created by the great number of substances having fingerprints in the THz region: innovative spectroscopic characterization of materials, opportunities to prevent and detect counterfeit products, precise control of tablet coatings and densities of active substances have been made possible thanks to THz technology [11–13].

In this perspective, THz microscopy can be identified as a potential diagnostic tool in many applications where a high spatial resolution is needed. Among existing techniques, confocal microscopy [14–16] is a very promising one, for it can sensibly reduce the depth of field of the microscope, as well as improve its resolution and contrast, proving very useful for inspection of close-by surfaces, where different planes have to be clearly distinguished, or where a depth information is crucial. Confocal microscopy at THz frequencies has been implemented for the first time only recently [17,18] with a maximum estimated lateral resolution as large as 310 μm and an axial resolution as deep as 400 μm.

The recent development of quantum cascade lasers (QCL) emitting at THz frequencies [19] should make a further improvement of THz imaging technologies possible, thanks to the avail-

#170679 - $15.00 USD Received 15 Jun 2012; revised 10 Aug 2012; accepted 15 Aug 2012; published 10 Sep 2012

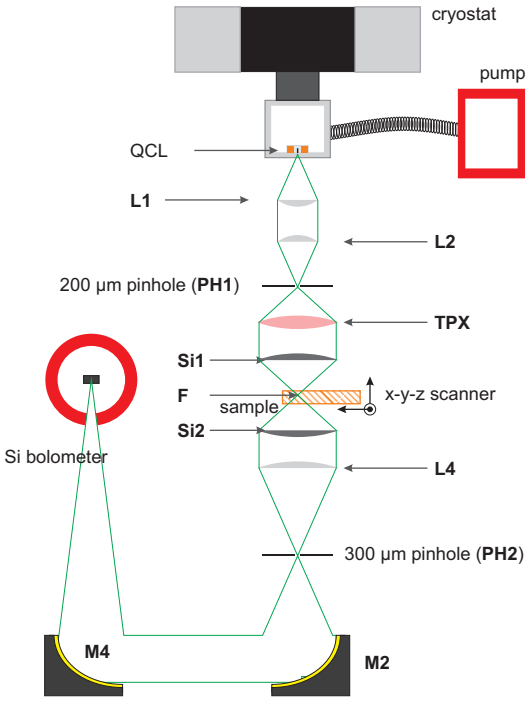

Fig. 1. Schematics of the final setup of the microscope. The lenses inserted are of different types: three Picarin lenses (**L1**, **L2**, **L4** with $NA \sim 0.447$), two Silicon lenses (**S1**, **S2** with $NA \sim 0.707$), a TPX lens (**TPX** with 0.447 numerical aperture) and two parabolic mirrors (**M2** with $NA \sim 0.447$ and **M4** with $NA \sim 0.167$ for a better coupling with the Si bolometer entrance window). The illustration highlights the differences among the various employed optics.

ability of a reliable, compact, and powerful laser source. For instance, QCLs have already been used to implement a differential scanning-aperture near-field microscopy set-up [20]. In the present work, we present a first confocal imaging system based on QCLs emitting at 2.9 THz and operating in a small-size cryogen-free Stirling cooler, achieving a lateral resolution better than $\sim 70\mu$m.

2. Experimental set-up

The experimental set-up is schematically depicted in Fig. 1. The employed QCL is based on a bound-to-continuum design for high injection efficiency (details of the device can be found in [21]). The device is mounted on the cold finger of a Stirling cryocooler (Ricor K535 Twin Piston Linear Integral Stirling Cryocooler) and maintained at a temperature of about 29 K. The QCL is driven at a current of 750 mA with 67.7 μs broad pulses and with an effective 50% duty cycle.

The profile of a QCL normally has an irregular shape due to the surface plasmon nature of the ridge waveguide modes. This is a relevant issue to be addressed for getting good performances out of the microscopy set-up since optical systems and components are normally designed for circular symmetry and gaussian beam shapes. As a consequence a spatial filter is necessary to obtain regular beam profiles: a metal pinhole (**PH1**) having a size of 200 μm was chosen in order to minimize power losses. Figures 2(a) and 2(b) show the comparison between the

#170679 - $15.00 USD Received 15 Jun 2012; revised 10 Aug 2012; accepted 15 Aug 2012; published 10 Sep 2012

shapes of the laser profile immediately after the cryostat and after the pinhole, respectively. A quantitative analysis of the QCL beam profile after **PH1** was performed by fitting the collected points with a gaussian function. The central cross sections (both horizontal and vertical) are shown in panels (c) and (d): the estimated divergence of the beam resulted in an angle $\theta \sim 50^{\circ}$ which is mainly due to the diffraction from the small aperture and in good agreement with the optical parameters of the system.

The first two identical Picarin lenses (**L1** and **L2**) collimate and focus the THz beam in **PH1**. The wavelength is about 103μm, hence diffraction is expected to be relevant; a large TPX lens is placed in front of the pinhole ensuring efficient collection of light from **PH1**. The first high numerical aperture Si lens (**Si1**) is inserted in order to focus light at point **F**, where the sample to image is scanned. The second Si lens (**Si2**) is placed at a distance of 50 mm; although these lenses help to maximize the system resolution, they also reduce the available sample space. A third large diameter (5 cm) Picarin lens (**L4**) is used to focus the light collimated by **Si2** into the second, confocal pinhole **PH2** (300 μm large). Light passing through **PH2** is directed to the liquid-He Si bolometer used as detector by a couple of parabolic mirrors (**M2** and **M4**). In particular, the last one matches the field of view of the entrance cone of the bolometer ensuring the maximum coupling efficiency.

The microscope images a single point of the sample at a time. A two-dimensional scan of the sample in the focus **F** results in a sharp image. Each pixel corresponds to a single sample region of the size of the central focus, while the corruption due to scattering from neighboring regions is minimized by the pinholes. In order to perform an automatic scan of the sample in each *cartesian* direction (*x*,*y* and *z*) a three dimensional moving stage is arranged by means of three motorized actuators and a software was expressly created for the purpose (employing a Labview graphical interface).

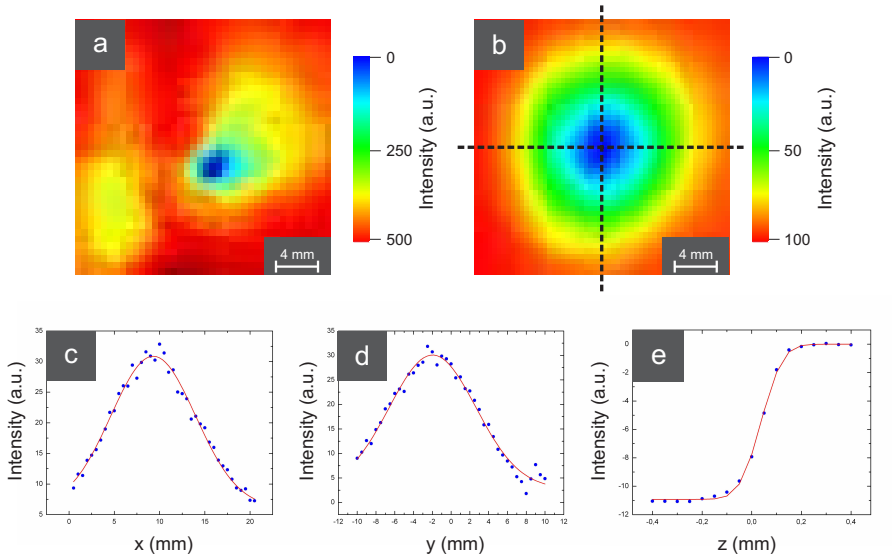

Fig. 2. Far field profile of the laser beam (a) at the output of the QCL (without filtering) and (b) after passing through the 200 μm pinhole: the measurements were performed by means of a pyroelectric detector mounted on a x-y moving stage at a distance of $\sim$ 2 cm; vertical (c) and horizontal (d) cross sections of the beam profile after the aperture are reported: fitting gaussian curves are shown in red. (e) Knife-edge scanning of the beam in the sample zone for the focal plane: the minimum measured waist is $\sim$ 132 μm

#170679 - $15.00 USD Received 15 Jun 2012; revised 10 Aug 2012; accepted 15 Aug 2012; published 10 Sep 2012

It is worth mentioning that a high level of precision is required in the alignment: the THz beam transmitted to the detector has indeed to pass through six lenses, two parabolic mirrors and two pinholes, meaning that a considerable amount of signal is lost along the optical path. The intensity of the radiation at the output of the QCL is few mW. The efficiency of the microscope is estimated to be lower than 0.1 % (without inclusion of the sample).

The resolution of the system was tested by means of the scanning knife-edge technique [22] which gives an estimated focus waist of 132 μm, that gives, according to the Rayleigh criterion, a lateral resolution of about 67 μm (Fig. 2(e)) and an axial resolution better than 400 μm.

3. Results and discussion

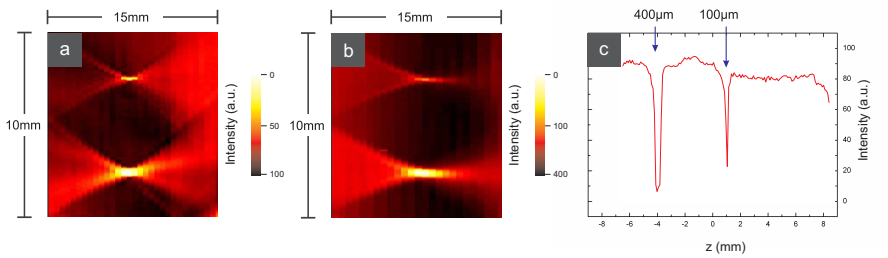

Fig. 3. Two-dimensional (2D) scan of the disk with two aluminum stripes, 400 μm and 100 μm wide respectively. The disk is oriented in order to keep the Al lines parallel to the *x* axis and perpendicular to the *z* axis. Pictures were captured with and without the 300 μm pinhole inserted in the setup ((a) and (b) respectively): each is 200x30 points. (c) Line scan in the focal plane: the 400 μm and 100 μm stripes correspond to the peaks indicated by the arrows.

In order to optimize an optical system, "ad hoc" test samples are needed: for the specific purpose we fabricated polyethylene (PE) disks having a thickness of 1.5 mm. These are transparent at THz frequencies and were used as substrate material for the subsequent deposition of either aluminum stripes (400 μm and 100 μm wide) or arrays of squares (400 μm large), evaporated by means of photo-lithographic techniques. A 2D scan of the stripes in the plane containing the optical axis and orthogonal to the stripes was performed in order to highlight the optical behavior at the sample position. The result is shown in Fig. 3. Images of the defocusing of the stripes were captured both with **PH2** inserted (Fig. 3(a)) and with no pinhole (Fig. 3(b)): the clearest points in the pictures correspond to the Al stripes in perfect focus. A clear improvement of the contrast is visible with **PH2** and the depth of field is also reduced. Panel (c) displays a section of panel (a) at the focal plane. The lateral dimensions of the 100 μm wide stripe are comparable to the resolution limit and therefore its image nearly provides a measurement of the point spread function of the system. To further highlight the effective advantages induced by the presence of the 300 μm pinhole in the setup, we performed a measurement of the defocusing of a test sample composed by two of the square-arrays disks, whose patterned surfaces were kept at a distance of 1.5 mm as illustrated in Fig. 4(a). Disks were rotated with respect to each other in order to avoid strongly overlapping images that would be difficult to interpret: squares on the first disk (the nearest one along the *z* axis to the QCL) were oriented in the vertical direction.

In Fig. 4 the comparison between the two cases is illustrated: the confocal images are depicted in the second row (panels (b), (c), and (d)), while the non-confocal ones are reported in the third one (panels (e), (f), and (g)) . Although the images at the bottom could appear, at first glance, clearer and of a better quality - because of the higher signal detected - the

#170679 - $15.00 USD Received 15 Jun 2012; revised 10 Aug 2012; accepted 15 Aug 2012; published 10 Sep 2012

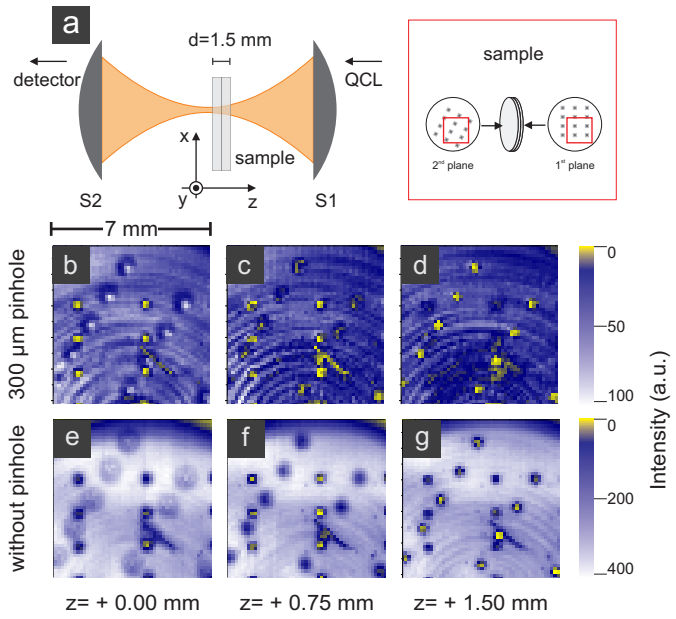

Fig. 4. (a) Schematics of the experimental arrangement employed for the confocal test of the optical system: two overlapping planes are involved in the measurements: the disks are separated by a distance of 1.5 mm and the whole sample is moved in the axial direction simulating the displacement of focus. ((b) to (d)) THz images of the object recorded in three positions along the optical axis: panel (a) shows the nearest plane with respect to the QCL, the other images were taken at steps of about 500 μm. The 300 μm pinhole was inserted. The *colormap* is chosen in order to demonstrate that the images from distant planes lay on different intensity levels. In the background some fringes are clearly visible: they are due to the circular surface roughness of the machined polyethylene substrate, which is not completely smooth. ((e) to (g)). The same measurements without confocal pinhole: note that here the resolution capability of the system is worse and it is not able to distinguish the fringes. The measured contrast between squares on the two planes is different in the two situations: $C_{confocal} = 0.84$ while $C_{non-confocal} = 0.27$.

measured contrast is unambiguously in favor of the confocal picture: $C_{confocal} = 0.84$ while $C_{non-confocal} = 0.27$.

In order to illustrate the high lateral resolution capability of the microscope on a real object, we employed a fresh green leaf. The main reason for this choice resides in the very high contrast achievable thanks to the presence of water in the very minute veins. A photograph of the sample under investigation is reported in Fig. 5(a). A first THz image of the entire sample was captured with 90x160 pixel resolution, with each point corresponding to a step 200 μm long. The result is depicted in Fig. 5(b). Next, we closed up on the area framed by the white rectangle and captured a picture at very high resolution (200x200 pixels, steps 50 μm long): the remarkable result is displayed in Fig. 5(c). The veins are highly defined and very small details are resolved.

In order to demonstrate the axial resolution capabilities, we chose to image two overlapping paper sheets. Some letters were written on these sheets using a pencil, because graphite possesses a good absorption at THz frequencies. In Figs. 5(d) and 5(e) the photographs of the two paper pieces are shown. To produce highly resolved THz images, we chose an area of 1.2 cm $\times$ 1 cm and the scan was performed at steps of 100 μm. The two sheets were then superimposed

#170679 - $15.00 USD Received 15 Jun 2012; revised 10 Aug 2012; accepted 15 Aug 2012; published 10 Sep 2012

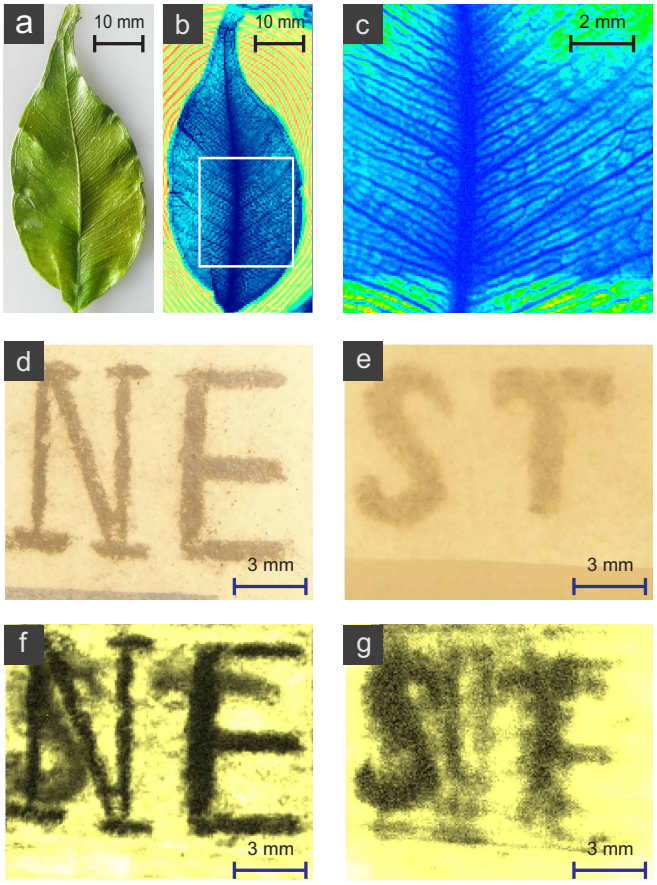

Fig. 5. (a) A photograph of a fresh leaf. (b) Confocal THz image of the same leaf with intensity levels referring to a wide chromatic range *colormap*, in order to highlight the veins. The measurements covered an area 1.8 mm x 3.2 mm and 90x160 pixels were recorded. (c) The rectangular white frame in panel (b) is imaged again with more points (200x200 pixels), in order to obtain a high resolution close-up of the leaf: the great amount of details shows the noteworthy capabilities of the instrument. (d,e) Photographs of two paper sheets which were subsequently superimposed at a distance of about 1.2 mm. Letters were written using a pencil. The left sheet is the nearest, along the optical axis, to the QCL. THz images of the paper sheets are shown in panels (f) and (g) with, respectively, the front and back plane in focus (120x100 pixels, linear *colormap*).

#170679 - $15.00 USD Received 15 Jun 2012; revised 10 Aug 2012; accepted 15 Aug 2012; published 10 Sep 2012

by keeping them fixed on the two sides of a blank, 1.2 mm thick, PE layer in order to ensure the parallelism between their surfaces. Figures 5(f) and 5(g) show the results. The plane with the letters *NE* was the nearest one to the laser source and this is the reason why it appears also as the clearest one. However, when the focus is shifted on the back plane, the letters on that sheet appear with enough contrast to be clearly distinguished. The *colormap* of the image is chosen in order to simulate the real object colors.

4. Conclusions

In the present work we assembled a confocal microscope exploiting a THz quantum cascade laser as light source: to our knowledge it is the first demonstration of a confocal setup employing a THz QCL. The confocal spatial filtering sensibly reduces the depth of field of the microscope, as well as improves its resolution and contrast. The images acquired indeed show unprecedented definition and an excellent capability of resolving planes located at different depths in the samples examined. Future evolutions of the present arrangement can be easily foreseen in order to expand the range of measurable objects. First of all the configuration can be modified to operate in reflection geometry, ensuring a higher signal-to-noise ratio and even higher depth resolution. Other relevant developments should be provided by the use of lasers emitting in continuous wave and specifically designed high-quality Si optics with good efficiency anti-reflection coating. Moreover the use of sources providing regular Gaussian beam profiles and a higher intensity [23] should also considerably improve the performances of the microscope.

Acknowledgments

We would like to thank the Istituto Sperimentale Italiano Lazzaro Spallanzani for its support through the Sessibov program, and the Istituto Superiore Mario Boella for the support through the Terafly project. We also acknowledge funding from MIUR through the FIRB Futuro in Ricerca Grant no. RBFR10LULP.

#170679 - $15.00 USD Received 15 Jun 2012; revised 10 Aug 2012; accepted 15 Aug 2012; published 10 Sep 2012